ACS POLYMERS Au
AN OPEN ACCESS JOURNAL OF THE AMERICAN CHEMICAL SOCIETY

pubs.acs.org/polymerau

Article

Transcending the Trade-off in Refractive Index and Abbe Number for Highly Refractive Polymers: Synergistic Effect of Polarizable Skeletons and Robust Hydrogen Bonds

Seigo Watanabe, Teru Takayama, and Kenichi Oyaizu*

Cite This: *ACS Polym. Au* 2022, 2, 458–466

Read Online

ACCESS | Metrics & More | Article Recommendations | Supporting Information

ABSTRACT: High-refractive-index polymers (HRIPs) are attractive materials for the development of optical devices with high performances. However, because practical components and structures for HRIPs are limited from the viewpoint of synthetic techniques, it has proved difficult using traditional strategies to enhance the refractive index (RI) of HRIPs to more than a certain degree (over 1.8) while maintaining their visible transparency. Here, we found that poly(phenylene sulfide) (**PPS**) derivatives featuring both methylthio and hydroxy groups can simultaneously exhibit balanced properties of an ultrahigh RI of n_D = 1.85 and Abbe number of ν_D = 20 owing to the synergistic effect of high molar refraction and dense intermolecular hydrogen bonds (H-bonds). This brand new strategy is anticipated to contribute to the development of HRIPs displaying ultrahigh RI with adequate Abbe numbers beyond the empirical n_D–ν_D threshold, which has not been achieved to date.

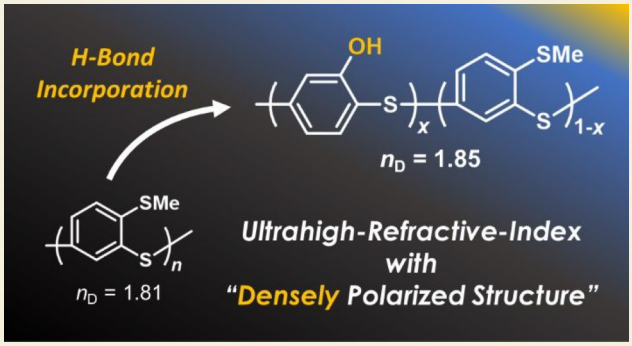

KEYWORDS: *Density, Hydrogen Bonds, Poly(phenylene sulfide), Sulfur Content, Ultrahigh Refractive Index*

INTRODUCTION

High-refractive-index polymers (HRIPs) have attracted worldwide attention in the field of optical devices from the viewpoint of enhancing performance and flexibility.[1−4] To date, numerous HRIPs bearing highly polarizable groups with a small volume (e.g., aromatics[5−7] and heteroatoms[8−14]) have been reported to display high refractive indices greater than 1.7. The desired refractive index (RI, n) values of optical polymers have been increased alongside the rapid development of photonic technologies; for example, transparent materials with RI values exceeding 1.8 are required for use as LED encapsulants in order to enhance the light extraction efficiency.[1] However, HRIPs displaying both ultrahigh RI values of over 1.8 and amorphous features have seldom been reported among optical polymers for visible-light usage. This can be ascribed to the relatively low polarity of the components of most organic polymers. Thianthrene-containing poly(phenylene sulfide) (**PPS**)[15] and triazine-bearing polymers[16] are among the few reported examples of HRIPs with RI values above 1.8 in the visible-light region. Selenium- or tellurium-containing polymers[17−19] and sulfur-rich polymers[20,21] have also been found to exhibit ultrahigh RI values exceeding 1.8 owing to their very high molar refraction ($[R]$). However, these polymers also displayed strong absorption bands in the near-UV−visible region, which led to coloration or low Abbe numbers (i.e., large chromatic aberration and low transparency) of the resulting films and limited their applications in this wavelength region. HRIPs with balanced properties (ultrahigh RI, thermostability, and adequate Abbe number) are required for outstanding optical materials.

As a solution to this problem, polymers with large numbers of short polysulfide chains synthesized by sulfur chemical vapor deposition of elemental sulfur using comonomers containing multiple vinyl groups were recently reported.[22,23] These polymers exhibited superior transparency and much higher RI values (up to n_D = 1.982, where D denotes the sodium D line at 589.3 nm)[23] compared to those of previously reported HRIPs, although the versatility of the synthetic route was limited by the need for vapor deposition. Therefore, the development of facile and versatile preparation methods for HRIPs with ultrahigh RI values, adequate Abbe numbers, and film formability has become a critical issue in the field.

We recently reported that the simultaneous incorporation of a backbone with a moderately high $[R]$ value and substituents

Received: June 28, 2022
Revised: August 8, 2022
Accepted: August 9, 2022
Published: August 19, 2022

https://doi.org/10.1021/acspolymersau.2c00030
ACS Polym. Au 2022, 2, 458–466

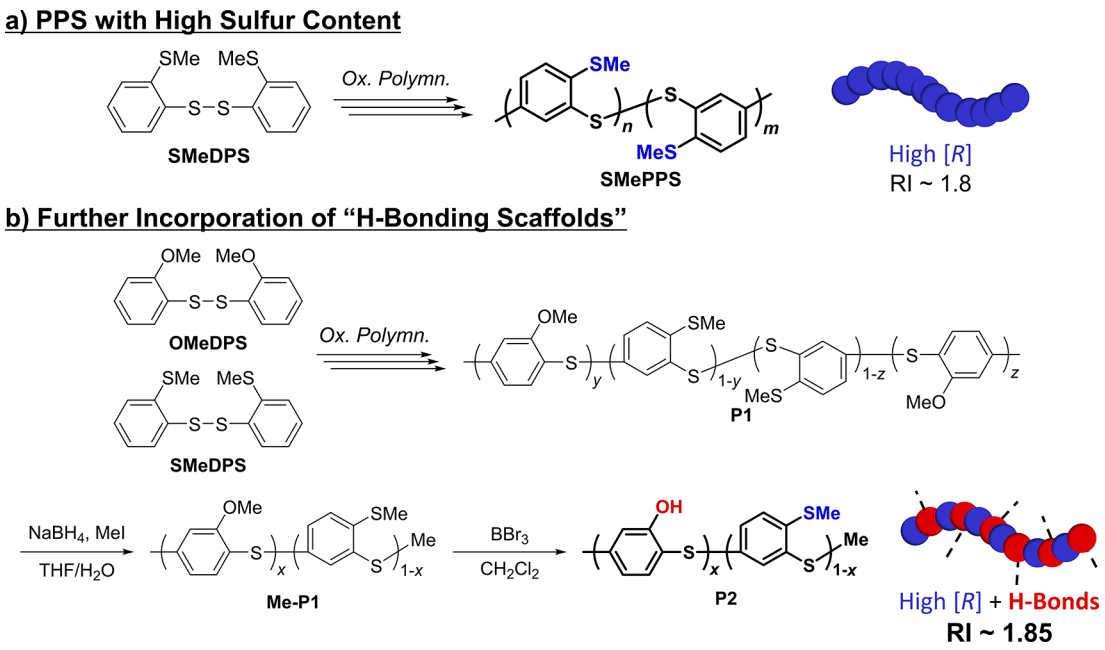

Figure 1. Concept of this study. (a) Synthesis of **SMePPS** through oxidative polymerization. (b) Further RI enhancement strategy enabled by the copolymerization with the H-bonding scaffold **OHPPS** leading to higher $[R]/V$ values.

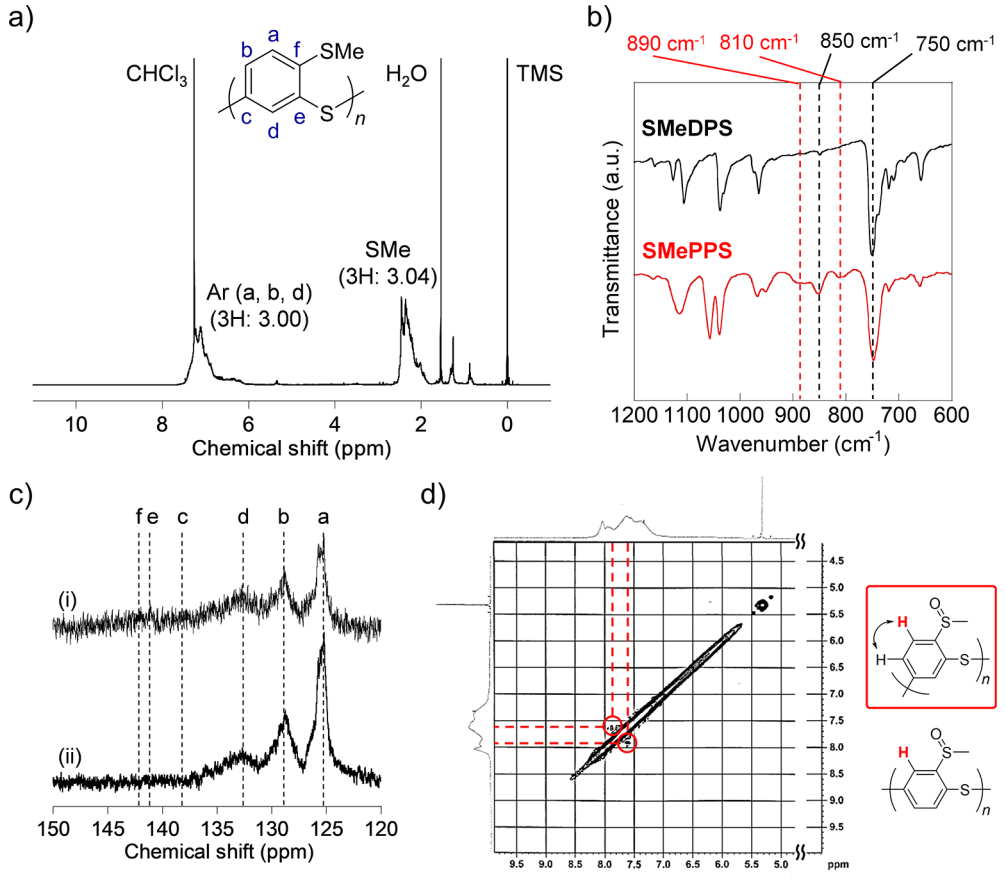

Figure 2. Synthesis of **SMePPS**. (a) ^{1}H NMR spectrum of **SMePPS** in chloroform-*d*. (b) IR spectra of **SMeDPS** and **SMePPS**. (c) (i) ^{13}C and (ii) ^{13}C-DEPT 135 NMR spectra of **SMePPS** in chloroform-*d*. (d) ^{1}H−^{1}H COSY spectrum of the sulfoxide-labeled **SMePPS**. The repeating structure was determined to be 2-methylthio-1,5-thiophenylene (structure circled by red square) owing to the correlation signals observed between the aromatic protons at the lowest field.

with hydrogen bonding (H-bonding) capability effectively afforded polymers with ultrahigh RI values without serious decline of Abbe numbers and transparency.[24] In particular, hydroxy-substituted **PPS** (**OHPPS**) exhibited an ultrahigh RI

https://doi.org/10.1021/acspolymersau.2c00030
ACS Polym. Au 2022, 2, 458−466

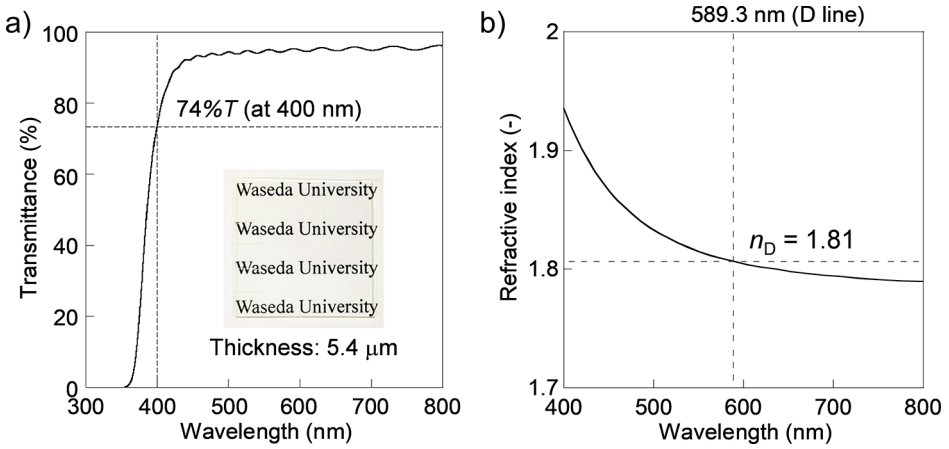

Figure 3. Optical properties of **SMePPS**. (a) UV−vis transmittance spectrum of an **SMePPS** thin film (inset: photograph of the film on a glass substrate). (b) Refractive index of **SMePPS** in the visible-light region. See Figure S6 for the detailed spectrum including extinction coefficient in the wider wavelength range.

(n_D = 1.80) with an Abbe number of ν_D = 20. Our detailed examination revealed that these superior properties originated from the effects of H-bonds between the side chains. Specifically, this unprecedented example was ascribed to the densely packed yet amorphous bulk polymer structure, affording a high RI with high molar refraction and low molecular volume (V).[24]

In this study, we further expand this proof-of-concept work toward a rational strategy for designing ultrahigh RI polymers, which enables breaking through the traditional empirical RI threshold as well as overcoming the typical trade-off between RI and Abbe number among organic polymers.

First, methylthio-substituted **PPS** (**SMePPS**) with a high sulfur content (42 wt %) was prepared as an ultrahigh-RI polymer (n_D = 1.81) with high polarizability (Figure 1a). Moreover, by introducing H-bonding scaffolds into the highly polarizable **PPS** chain through copolymerization with **OHPPS** (Figure 1b), the RI was further enhanced to n_D = 1.85 with an Abbe number of ν_D = 20. To the best of our knowledge, this is the first reported example of HRIPs simultaneously displaying such an ultrahigh RI and adequate Abbe number, which exceeded the empirical n_D−ν_D threshold. The synergistic effect of high polarizability and intermolecular H-bonds was revealed to be effective for maximizing the RI by increasing the $[R]/V$ values, which was also quantitatively demonstrated by investigation of the bulk structure and properties.

RESULTS AND DISCUSSION

Oxidative Polymerization of Bis(2-methylthiophenyl) Disulfide

First, methylthio-substituted **PPS** (**SMePPS**) was synthesized through the oxidative polymerization of bis(2-methylthiophenyl) disulfide (**SMeDPS**). The **SMeDPS** monomer was prepared via Grignard reaction of 1-bromo-2-thioanisole and subsequent oxidation of the thiol, affording yellow needle-like crystals. The structure of **SMeDPS** was confirmed by ^{1}H NMR, ^{13}C NMR, and FAB-MS spectra (see the experimental procedure and Figure S1). Owing to the oxidation feasibility of **SMeDPS**, as confirmed by the presence of an irreversible oxidation peak at 1.56 V vs Ag/AgCl in the cyclic voltammogram (Figure S2), the oxidative polymerization of **SMeDPS** proceeded with either oxygen with the VO(acac)$_2$−H$^+$ redox catalyst[25] or 2,3-dichloro-5,6-dicyano-1,4-benzoquinone (DDQ)[26] as the oxidant. The reaction behavior and polymer structure were investigated through various spectroscopic measurements and density functional theory (DFT) calculations. The linear structure with two carbon−sulfur bonds per one unit was confirmed from the ^{1}H NMR spectrum, in which the signals corresponding to the aromatic and methylthio protons were detected with the same integrals (Figure 2a). From the IR spectrum of the polymer, the presence of 1,2,4-substituted phenylene moieties was verified from not only the absorption bands at 750 and 850 cm^{-1}, which were derived from the terminal 1,2-substituted phenylene, but also the newly observed bands at 810 and 890 cm^{-1} after the polymerization (Figure 2b). Therefore, in the oxidative polymerization of **SMeDPS**, the chain-growth reaction (i.e., the electrophilic substitution of the sulfonium electrophile and the sulfide monomer/oligomer) dominantly proceeded at the 4- or 5-position to the carbon−sulfur bonds on the benzene ring. The ^{13}C and ^{13}C-DEPT NMR spectra of the polymer revealed six kinds of aromatic carbons, three of which were assigned as carbons with C−H bonds, indicating the obtained polymer was composed of a single structure with trisubstituted aromatic rings (Figure 2c). Because of the similar electromagnetic features of the aromatic protons and carbons adjacent to the methylthio-substituted carbons and the arylene sulfide-substituted carbons, these signals were indistinguishable in the ^{1}H and ^{13}C NMR spectra. Therefore, we further converted only the methylthio substituents to S═O moieties by *m*CPBA oxidation to separate the two peaks. In the ^{1}H−^{1}H COSY spectrum of the sulfoxide-labeled polymer, a ^{1}H−^{1}H correlation was observed between the aromatic proton signals at 7.9 and 7.6 ppm, indicating that this pair of adjacent aromatic protons was located just next to the labeled sulfoxide (Figure 2d), and therefore, the structure of **SMePPS** was finally determined as that of poly(2-methylthio-1,5-phenylenesulfide). The DFT calculation results for **SMeDPS** also demonstrated Friedel−Crafts reactivity of the carbon at the 5-position higher than that at the 4-position, as confirmed by the presence of both a more distributed HOMO and more negative Mulliken charge of the carbon at the 5-position (Figure S3).

The molecular weight of **SMePPS** remained relatively low (up to M_w = 2.3 × 10^3) according to size exclusion chromatography (SEC) measurements (Table S1). Owing to

https://doi.org/10.1021/acspolymersau.2c00030
ACS Polym. Au 2022, 2, 458−466

the relatively low oxidation potential of **SMeDPS** among **PPS** derivatives, the monomer was instantly oxidized in the early stage of the reaction, and the subsequent electrophilic substitution (corresponding to chain propagation) can be defined as the rate-determining step. Indeed, the polymerization proceeded better in a low-donor-number solvent at low concentration but remained with small M_w values, suggesting that the low molecular weight of the polymers was ascribed to not the solubility of the polymers but the lower Friedel−Crafts reactivity of **SMeDPS** compared to that of other DPS monomers.[27] The rigidity and high steric hindrance of the 1,5-disubstituted oligomeric structure during the electrophilic attack ultimately affected low reactivity, which finally resulted in low molecular weight for **SMePPS**.

Thermal and Optical Properties of SMePPS

Next, the outstanding thermal and optical performances of **SMePPS** were confirmed from various measurements. The differential scanning calorimetry (DSC) thermogram of **SMePPS** revealed high thermal stability with single glass-transition behavior in a suitable temperature window (up to T_g = 103 °C) (Figure S5a inset). The X-ray diffraction (XRD) profile also revealed no crystalline peaks derived from pristine **PPS**, indicating the completely amorphous nature of **SMePPS** owing to the steric effects associated with the bulky methylthio substituents (Figure S5a). Thermogravimetric analysis (TGA) of **SMePPS** indicated a high thermal degradation temperature of T_{d5} = 319 °C, which is similar to the reported values for other **PPS** and its derivatives obtained by oxidative polymerization (Figure S5b).[14,27] On the basis of these superior properties as an optical material with high processability and good solubility, thin films of **SMePPS** were fabricated on glass and Si substrates to investigate the optical properties. The **SMePPS** films showed visible transparency with a transmittance of >74%T for a thickness of 5.4 μm (normalized transmittance: > 94%T for 1 μm thickness) (Figure 3a). This was ascribed to the dispersed nature of the sulfur atoms as sulfide bonds rather than polysulfides,[22] which may cause film coloration (Figure 3a), although the transparency was lower than that for **OHPPS** with a similar RI (n_D = 1.80).[24] This decrease in transparency was also confirmed by the larger extinction coefficient of **SMePPS** compared to that with other alkyl-, alkoxy-, or hydroxy-substituted **PPS** in the near-UV region owing to its abundance of highly polarizable sulfur atoms (42 wt %) (Figure S6). Furthermore, **SMePPS** exhibited an ultrahigh RI of n_D = 1.81 and an Abbe number of ν_D = 19, the former of which especially represents the highest among the **PPS**-derived homopolymers to the best of our knowledge (Figure 3b). Increasing $[R]$ through the introduction of short sulfide side chains, which also served as a source for steric effects affording amorphous bulk film, was thus demonstrated to be an effective strategy for enhancing the RI of **PPS** derivatives while maintaining an adequate Abbe number.

Synthesis of Hydroxy- and Methylthio-Substituted Copolymers (P2)

Next, we anticipated that the RI of **SMePPS** could be further enhanced by decreasing the free volume through the introduction of hydroxy-substituted **PPS** (**OHPPS**) moieties as a copolymerization unit, which can contribute to realizing higher $[R]/V$ values.[24] First, copolymers composed of **SMePPS** and **OMePPS** units (**P1**) were synthesized through the oxidative polymerization of **SMeDPS** and **OMeDPS** to serve as precursors for yielding copolymers with **SMePPS** and **OHPPS** units (**P2**) (Figure 1b). Three kinds of **P1** with different composition ratios were prepared to investigate the effect of introducing the methoxy and hydroxy groups into the polymer sequence on the RI values (Table S4). The DOSY NMR spectra of **P1** confirmed the presence of copolymerized products, as demonstrated by the same diffusion coefficient for all the signals corresponding to each unit (Figure S7). The IR spectra of **P1** also revealed the presence of 1,2,4-substituted benzene rings ($\delta_{C-H\ (Ar)}$: 810 and 900 cm^{-1}) and terminal 1,2-substituted benzene rings ($\delta_{C-H\ (Ar)}$: 750 and 840 cm^{-1}), indicating that each unit was successfully incorporated as in the case of **OMePPS**[27] and **SMePPS** (vide supra) (Figure S8). We also checked the copolymerization kinetics in the system containing the same number of equivalents of fed monomers (Figure S9). The molecular weight of the product increased drastically over the first hour before increasing more gradually (Figure S9a,b). Therefore, the copolymerization proceeded according to a step-growth mechanism in the early stage of the reaction, whereas disulfide exchange and coupling reactions of the oligomeric products appeared to be the major reactions in the middle and latter stages. The reactivity of each monomer was almost identical from the perspective of oxidation potential (E_{ox} = 1.56 V for **SMeDPS** and 1.58 V for **OMeDPS**),[27] resulting in an almost constant composition ratio x with values close to the theoretical ones (x_{theo} = 0.5) during the polymerization progress (Figure S9e). Consequently, a series of **P1** were afforded as nearly ideal random copolymers. On the other hand, **OMePPS−PPS** copolymers obtained by oxidative polymerization were gradient-like polymers, which was confirmed from the larger introduction rate of **OMePPS** unit (see black dots on Figure S9e for the DDQ oxidant system, and see our previous report[24] for the O_2/VO(acac)$_2$-H$^+$ system). Due to the randomly incorporated sequence during the copolymerization for **P1** synthesis, the oligomers of **P1** were highly soluble until the later stage of polymerization and the termination of polymerization was also prevented. Although the molecular weight of **P1** still remained in small values of $M_w \sim 10^3$, higher Friedel−Crafts reactivity and p-selectivity of the **OMeDPS** counterpart prolonged the polymerization and resulted in higher M_w values than **SMePPS**.

Finally, the target copolymers consisting of **OHPPS** and **SMePPS** units (**P2**) were prepared via postpolymerization modification of **P1**, according to the same strategy described in our previous report.[24] First, the disulfide bonds in the main chain of **P1** were functionalized to obtain methyl-terminated **P1** (**Me-P1**) beforehand for preventing the simultaneous occurrence of disulfide cleavage and demethylation of methoxy groups (Table S5).[24] Although the ^{1}H NMR signal corresponding to the terminal methyl group was observed in the same region as those of the methylthio substituents and could not be detected independently, the progress of the end-functionalization was confirmed from the increased integral ratio of the broad peak near 2.4 ppm in the spectra of **Me-P1** with respect to that of **P1** (Figure S10). No newly observed peaks were detected in the IR spectra after end-functionalization and **Me-P1** contained no structural defects (Figure S11). The degree of end-functionalization was greater than 88%, determined by comparison of the M_n values from the NMR and SEC measurements. The lower M_n and M_w values of **Me-P1** compared with **P1** indicated that the disulfide bonds of **P1** were located not only at the terminus but also within the polymer chains. The subsequent demethylation of **Me-P1** also

https://doi.org/10.1021/acspolymersau.2c00030
ACS Polym. Au 2022, 2, 458−466

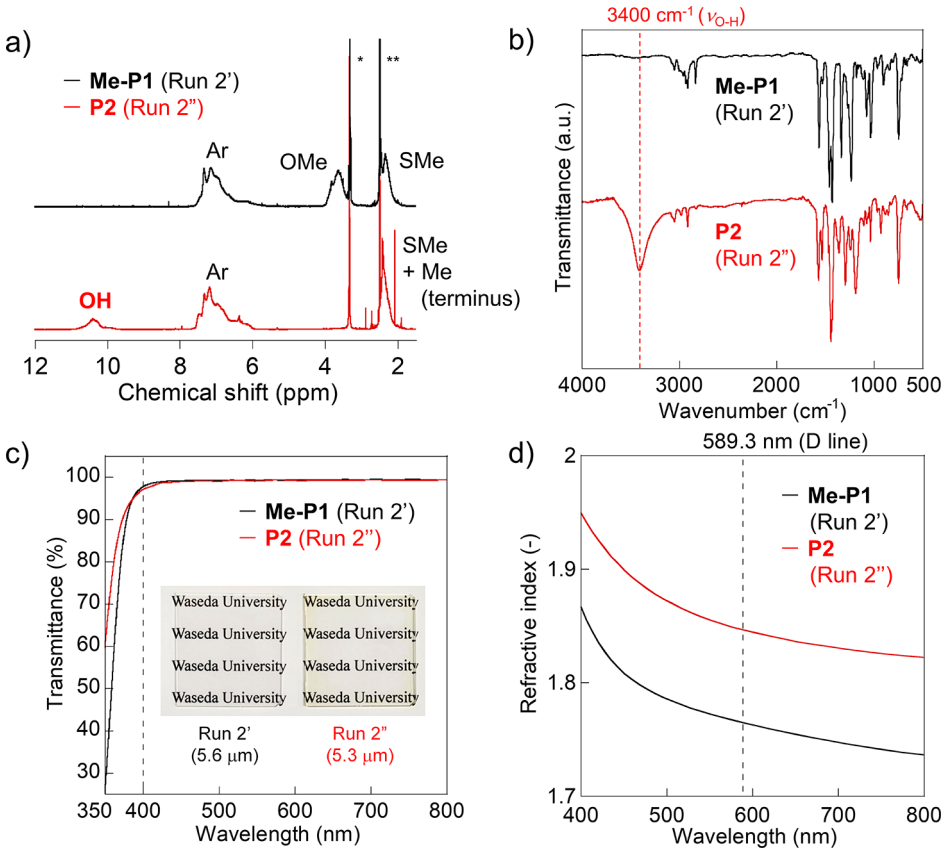

Figure 4. Synthesis and properties of **P2**. (a) ^{1}H NMR spectra of **Me-P1** (run 2′) and **P2** (run 2″) in DMSO-d_6. (b) IR spectra of **Me-P1** (run 2′) and **P2** (run 2″). (c) UV−vis spectra of **Me-P1** and **P2** thin films (thickness was normalized to 1 μm). Inset: thin films of **Me-P1** (run 2′) and **P2** (run 2″). (d) Refractive indices of **Me-P1** and **P2**.

proceeded efficiently with high conversions (≥93%), as monitored through the corresponding peak changes in the ^{1}H NMR and IR spectra (Figure 4a,b and Figures S12 and S13). **P2** was finally obtained without any degradation, as confirmed by the similar M_n values before and after the demethylation (Table S6). However, the bulk properties of the **PPS** derivatives, i.e., molecular weight, mechanical properties, and melt processability, should be further improved for practical applications. We have currently been focusing on these remaining issues by means of engineering the reactive disulfide bond in the **PPS** chains, which can be accomplished through the end-functionalization using multiarm modification agents, disulfide metathesis, or other transformation reactions (e.g., click reactions) as chain-extension techniques.[28−30]

Crystalline and Thermal Properties of Copolymers

The amorphous natures of **Me-P1** and **P2** were revealed from their XRD profiles, irrespective of the x values and the presence/absence of hydroxy groups (Figure S14). Even after the introduction of the H-bonds, the random sequence of each unit and the efficiency of plausible intermolecular interactions other than H-bonds between hydroxy groups (e.g., H-bonds involving methylthio groups as acceptors, S−π interactions of the aromatic rings and methylthio groups, and π−π interactions between the aromatic rings) contributed to the amorphous nature of **P2**. In addition, the bulkiness of the 1,5-substituted phenylene units compared with 1,4-substituted units presumably assisted with the amorphous structures of **Me-P1** and **P2**.

According to the DSC thermograms, a single glass transition for **P1**, **Me-P1**, and **P2**, which was same as the case for **OHPPS-PPS** copolymers, suggested a homogeneous bulk structure in a molecular level. The T_g values of **P1** were increased according to larger x values owing to the higher T_g of **OMePPS** (T_g = 105−132 °C)[27] compared with **SMePPS**; this trend of T_g versus x was retained for the series of **Me-P1** (Figure S15a). However, the T_g values of **P2** were slightly lower than those of the corresponding **Me-P1**, contrary to the expected effect of H-bonds described above. This trend was similar to that observed for the demethylation of **OMePPS−PPS** copolymers but distinct from that for **OMePPS**, which makes T_g higher.[24] The random sequence of **P2** was the key to decreasing T_g owing to its lower rotational barrier than **Me-P1**, whose effect exceeded the binding effect of polymer chains through H-bonds.

Optical Properties of Copolymers

Finally, the influence of the sulfur and hydroxy contents on the optical properties was investigated. **Me-P1** and **P2** were more transparent in the visible region (over 96%T for 1 μm thickness) than **SMePPS** owing to their lower contents of highly polarizable sulfur atoms, preventing excessive interactions involving sulfide moieties in the bulk state (Tables 1 and S7). Additionally, higher transparency of **P2** than **OHPPS-PPS** copolymers[24] held the difference of microstructures in the bulk state, suggesting that **P2** had more homogeneous structure with less clustering of particular segments and optical scattering would have been prevented. The smaller solution absorptivity of **P2** compared with **SMePPS** also contributed to

https://doi.org/10.1021/acspolymersau.2c00030
ACS Polym. Au 2022, 2, 458−466

Table 1. Optical Properties and Density of P2

run	polymer	x^a (−)	%T[b] at 400 nm	n_D[c] (−)	ν_D[c] (−)	density[d] (g cm^{-3})
	SMePPS	0	94	1.81	19	1.39
1″	**P2**	0.27	97	1.80	16	1.39
2″	**P2**	0.53	97	1.85	20	1.48
3″	**P2**	0.77	96	1.83	17	1.47
	OHPPS	1.00	97[e]	1.80[e]	20[e]	1.50[e]

[a]Determined by ^{1}H NMR. [b]Determined by UV−vis spectroscopy (normalized values for a thickness of 1 μm). [c]Determined by spectroscopic ellipsometry. [d]Determined by a dry density meter (the values were density for powder samples). [e]Values from ref 24.

the higher transparency of the polymers mainly derived from their inherent structures (Figure S19), which was ascribed to the small number of lone pairs and polarizable atoms adjacent to the aromatic rings.[14] Focusing on the properties through the demethylation, the transparency of **P2** was slightly decreased in the bulk state but increased in diluted solution (Figure 4c and Figures S20 and S21), which was a different trend from those of **Me-OMePPS** and **OHPPS**.[24] Therefore, plausible intermolecular interactions involving methylthio groups as acceptors, such as H-bonds and S−π interactions, apparently occurred in the bulk films of **SMePPS** and **P2**, leading to their low visible transparency. The RI values of **SMePPS**, **P1**, and **Me-P1** decreased upon the introduction of methoxy groups in accordance with the decreased average molar refraction per repeating unit (black lines in Figures 4d and S23). After the demethylation, **P2** displayed RI values larger than those of the corresponding **Me-P1** owing to the more compact skeleton (red lines in Figures 4d and S23). Furthermore, the differences in n_D were small (∼0.02) in the low-x region (run 1″) but larger (∼0.08) in the large-x region (runs 2″ and 3′′), although the Abbe numbers (ν_D) were maintained with values of approximately 20 irrespective of the x values (Figure 5a). This difference was attributable to the number of H-bonds, whose effect on lowering the free volume was exerted only in the bulk state with the densely incorporated H-bonds. Furthermore, the relationship between the x and n_D values of **P2** was anomalous: the change in RI was not proportional to x and the maximum n_D of 1.85 was observed at the intermediate composition (x = 0.53, run 2″) (Figure 5a and Table 1). In general, the RI values of bicomponent copolymers change monotonically following additivity rules and decrease as the composition ratio of the unit with small [R] increases, similar to that in the previous report;[31] the n_D values of **Me-P1** changed with x according to this trend. However, this empirical rule was not applicable to the **P2** system owing to the unusual bulk structure derived from the H-bonding effect induced by the **OHPPS** units.

Synergistic Effect of Molar Refractivity and Intermolecular Interactions

To elucidate the mechanism underlying the anomalous relationship between the RI and composition ratio of **P2**, the bulk properties of **P2** were further investigated. First, the density of **P2** was measured for each x value to examine the H-bonding effect, for the density of a polymer is directly related to its free volume.

P2 with a small x value (run 1″, x = 0.27) exhibited almost the same density as **SMePPS**, whereas the density of **P2** with larger x values (run 2″, x = 0.53, and run 3″, x = 0.77) displayed remarkably high densities similar to that of **OHPPS**

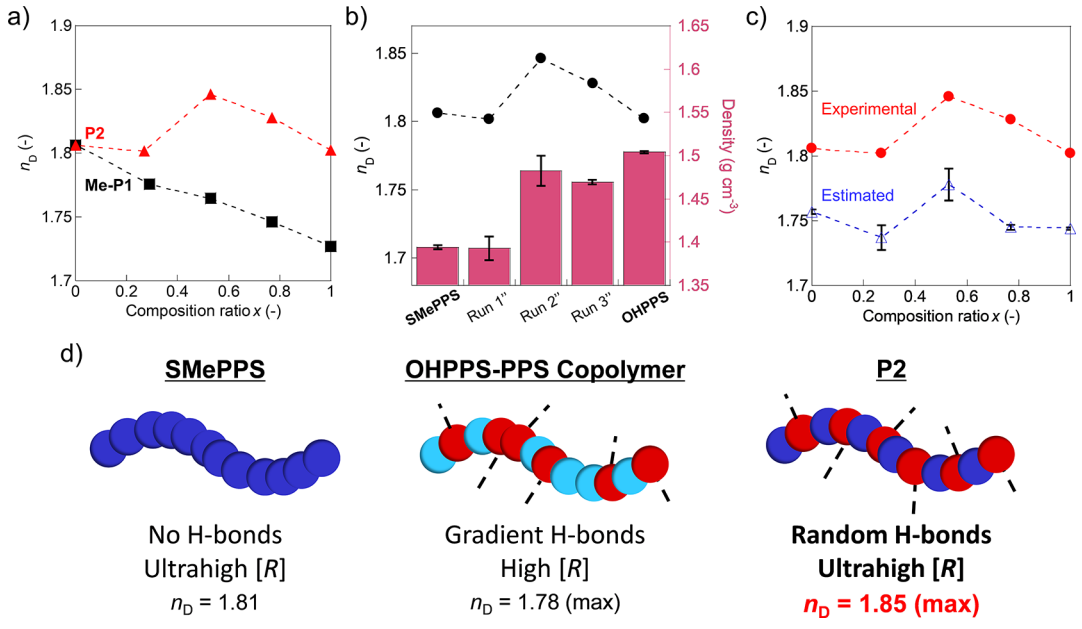

Figure 5. RI changes for **Me-P1**, **P2**, and homopolymers depending on the methoxy/hydroxy content. Values for **OMePPS** (**Me-P1** with x = 1.00) and **OHPPS** (**P2** with x = 1.00) were referred from the previous reports (refs 27 and 24, respectively). (a) Relationship between composition ratio and experimental n_D for **Me-P1** (black squares) and **P2** (red triangles) (before and after demethylation). (b) Experimental n_D (line graph) and density (bar charts) for **SMePPS**, **OHPPS**, and **P2**. The error bars indicate the standard deviation of the density measurements (average of five times). (c) Estimated (blue open triangles) and experimental (red circles) n_D values for **SMePPS**, **OHPPS**, and **P2** at each composition ratio. The error bars indicate the standard deviation of the estimated RI values, which were in accordance with the deviation of the density measurements. (d) Schematic comparison of H-bond distribution, [R] values, and n_D values for **SMePPS**, **OHPPS**−**PPS** copolymer,[24] and **P2**. The blue and red circles represent high-[R] moieties and H-bonding moieties, respectively, and the dotted lines represent intermolecular H-bonds. The color depth of the blue circles represents the magnitude of the [R] values.

https://doi.org/10.1021/acspolymersau.2c00030
ACS Polym. Au 2022, 2, 458−466

(1.50 g cm^{-3}) (Figure 5b).[24] This trend was in accordance with the sharp enhancement of RI in the case of **P2** from run 1″ to run 2″. These results suggested that the introduced H-bonds markedly lowered the free volume in the case of **P2** with moderate to high hydroxy contents, which led to the synchronized RI enhancement in this system. To estimate the precise RI values taking the contributions of the $[R]$ and V changes into account, we also estimated n_D values for each x through the Lorentz−Lorenz equation, by adopting measured densities and calculated molar refractions (Figure 5c). The estimated n_D values (blue data points in Figure 5c) followed the same trend as the experimental values (red data points in Figure 5c) with increasing number of hydroxy groups, suggesting that the experimental RI values varied in accordance with the change in $[R]/V$ values. The deviations of the estimated RI values from the experimental ones were ascribed to the more densely packed structure of the polymers in the bulk (film) states compared with the powder states (the density of powder samples was adopted as an alternative to that of films in this study, owing to the difficulty associated with preparing free-standing films). Because the polymer chains were less densely packed in the powder state than in the bulk state on account of the higher concentration of voids and boundaries, which resulted in a smaller number of neighboring polymer chains,[32] the **P2** films would be expected to display higher densities than the powder samples, implying higher experimental RI values in the bulk system. By comparing the IR spectra of **P2** before and after film fabrication, the O−H stretching vibrations involving H-bonds were found to shift to lower wavenumbers (Figure S24), indicating the presence of H-bond networks with a more dense and homogeneous distribution in the **P2** bulk films.

In our previous study,[24] we reported that copolymers composed of **OHPPS** and unsubstituted **PPS** (termed **OHPPS−PPS** copolymers hereafter) exhibited lower RI values than **OHPPS**; however, in this study, **P2** showed RI values higher than those of both **OHPPS** and **SMePPS**. This difference suggests that the RI values of **OHPPS** and its copolymers are strongly dependent on the sequence, the $[R]$ values of each component, and the content of hydroxy-substituted moieties (Figure 5d). Although **OHPPS−PPS** copolymers were obtained with gradient-like sequences and therefore the hydroxy groups were randomly and sparsely incorporated, **P2** were random copolymers with homogeneous distributions of hydroxy groups. In particular, the randomness of the **P2** sequence was the highest for the composition ratio of $x \sim 0.5$ owing to the approximately equivalent incorporation of each unit in the copolymer. The above difference in the unit distribution depends on the reactivity of the monomers toward disulfide oxidation and Friedel−Crafts substitution, both of which are defined as elementary reactions during the oxidative polymerization.[26] Because the introduction of electron-donating groups to a DPS monomer is effective for both lowering the oxidation potential (E_{ox}) and enhancing the electrophilic substitution of the sulfonium cation, the oxidative copolymerization of **OMeDPS** with another DPS monomer having a similar oxidation potential is effective for obtaining nearly random copolymers with homogeneously distributed H-bonding sites. Furthermore, the higher $[R]$ values of the **SMePPS** unit compared with the **PPS** unit partially resulted in different RI changing trends in the system. Taking this hypothesis into account, the synergistic effect of high $[R]$ and H-bonds would lead to an RI enhancement in the case of copolymers composed of **OHPPS** and another **PPS** unit if the latter unit satisfies the following conditions: (1) a higher $[R]$ value than the **OHPPS** unit (contributing to higher unit refractivity) and (2) an E_{ox} value of the corresponding DPS monomer close to that of **OMeDPS** (affording random sequences). The preparation of **OHPPS**-incorporated PPS copolymers (**OHPPS−PPS** copolymers, **P2**, etc.) possessing various sequences, which would be enabled by the development of a precisely controlled oxidative polymerization strategy, and investigation of their optical properties will be among the key objectives for our future work to expand this RI enhancement strategy.

CONCLUSION

A series of ultrahigh-refractive-index **PPS** derivatives bearing both hydroxy and methylthio groups were synthesized by means of postpolymerization modification of the methyl-protected precursors. These copolymers exhibited higher RI values (up to n_D = 1.85) than the corresponding homopolymers while maintaining adequate Abbe numbers ($\nu_D \sim 20$), owing to the synergistic effect of highly polarizable groups and densely incorporated robust H-bonds. This mechanism was also elucidated from a classical perspective using the Lorentz−Lorenz equation, revealing that the dual incorporation of methylthio and hydroxy groups enhanced the $[R]/V$ values of the polymer on the macroscopic scale, leading to higher refractivity. Practically, these superior optical properties are notable among the previously reported polymers including other **PPS** derivatives (Figure S25). To the best of our knowledge, this copolymer system is the first example that enhances RI through the copolymerization of each component. This novel strategy is expected to be applicable to the design of not only **PPS** derivatives but also various other promising HRIP candidates to realize ultrahigh RI values with adequate Abbe numbers beyond the empirical n_D−ν_D threshold.

ASSOCIATED CONTENT

Supporting Information

The Supporting Information is available free of charge at https://pubs.acs.org/doi/10.1021/acspolymersau.2c00030.

Synthetic and experimental procedures, data for oxidative polymerization and postpolymerization modification, additional thermal/optical properties, calculation details for the RI estimation (PDF)

AUTHOR INFORMATION

Corresponding Author

Kenichi Oyaizu − *Department of Applied Chemistry and Research Institute for Science and Engineering, Waseda University, Shinjuku-ku, Tokyo 169-8555, Japan;* orcid.org/0000-0002-8425-1063; Email: oyaizu@waseda.jp

Authors

Seigo Watanabe − *Department of Applied Chemistry and Research Institute for Science and Engineering, Waseda University, Shinjuku-ku, Tokyo 169-8555, Japan;* orcid.org/0000-0002-0498-8330

Teru Takayama − *Department of Applied Chemistry and Research Institute for Science and Engineering, Waseda University, Shinjuku-ku, Tokyo 169-8555, Japan*

https://doi.org/10.1021/acspolymersau.2c00030
ACS Polym. Au 2022, 2, 458−466

Complete contact information is available at:
https://pubs.acs.org/10.1021/acspolymersau.2c00030

Author Contributions

S.W., T.T., and K.O. conceived and designed the experiments. S.W. and T.T. performed the experiments and calculations. S.W. and K.O. wrote the manuscript. K.O. supervised the project. All authors analyzed the data, discussed on the results and the written manuscript, and have given approval to the final version of the manuscript. S.W. and T.T. contributed equally to this work.

Notes

The authors declare no competing financial interest.

■ ACKNOWLEDGMENTS

This work was partially supported by Grants-in-Aid for Scientific Research (Nos. 18H05515 (K.O.), 21H04695 (K.O.), and 22J11820 (S.W.)) of MEXT, Japan. S.W. acknowledges the support by Waseda Research Institute for Science and Engineering, Grant-in-Aid for Young Scientists (Early Bird). A part of this work was supported by Advanced Research Infrastructure for Materials and Nanotechnology in Japan (ARIM) of MEXT and was also the result using research equipment (ECX-500, AVANCE III 600, JMS-GCMATE II, RINT-UltimaIII, and TG8120: Material Characterization Central Laboratory) shared in MEXT Project for promoting public utilization of advanced research infrastructure (program for supporting construction of core facilities) Grant No. JPMXS0440500021. The authors thank Dr. Kan Hatakeyama-Sato (Waseda Univ.) for assistance with DFT calculations.

■ REFERENCES

(1) Liu, J. G.; Ueda, M. High Refractive Index Polymers: Fundamental Research and Practical Applications. *J. Mater. Chem.* **2009**, *19* (47), 8907−8919.

(2) Higashihara, T.; Ueda, M. Recent Progress in High Refractive Index Polymers. *Macromolecules* **2015**, *48* (7), 1915−1929.

(3) Kleine, T. S.; Glass, R. S.; Lichtenberger, D. L.; Mackay, M. E.; Char, K.; Norwood, R. A.; Pyun, J. 100th Anniversary of Macromolecular Science Viewpoint: High Refractive Index Polymers from Elemental Sulfur for Infrared Thermal Imaging and Optics. *ACS Macro Lett.* **2020**, *9* (2), 245−259.

(4) Lee, T.; Dirlam, P. T.; Njardarson, J. T.; Glass, R. S.; Pyun, J. Polymerizations with Elemental Sulfur: From Petroleum Refining to Polymeric Materials. *J. Am. Chem. Soc.* **2022**, *144* (1), 5−22.

(5) Liu, J.-G.; Nakamura, Y.; Shibasaki, Y.; Ando, S.; Ueda, M. Synthesis and Characterization of Highly Refractive Polyimides from 4,4′-Thiobis[(*p*-Phenylenesulfanyl)Aniline] and Various Aromatic Tetracarboxylic Dianhydrides. *J. Polym. Sci. Part A Polym. Chem.* **2007**, *45* (23), 5606−5617.

(6) Terraza, C. A.; Liu, J.-G.; Nakamura, Y.; Shibasaki, Y.; Ando, S.; Ueda, M. Synthesis and Properties of Highly Refractive Polyimides Derived from Fluorene-Bridged Sulfur-Containing Dianhydrides and Diamines. *J. Polym. Sci. Part A Polym. Chem.* **2008**, *46* (4), 1510−1520.

(7) Nakagawa, Y.; Suzuki, Y.; Higashihara, T.; Ando, S.; Ueda, M. Synthesis of Highly Refractive Poly(Phenylene Thioether)s Containing a Binaphthyl or Diphenylfluorene Unit. *Polym. Chem.* **2012**, *3* (9), 2531.

(8) Nakano, K.; Tatsumi, G.; Nozaki, K. Synthesis of Sulfur-Rich Polymers: Copolymerization of Episulfide with Carbon Disulfide by Using [PPN]Cl/(Salph)Cr(III)Cl System. *J. Am. Chem. Soc.* **2007**, *129* (49), 15116−15117.

(9) You, N.-H.; Suzuki, Y.; Yorifuji, D.; Ando, S.; Ueda, M. Synthesis of High Refractive Index Polyimides Derived from 1,6-Bis(*p*-Aminophenylsulfanyl)-3,4,8,9-Tetrahydro-2,5,7,10-Tetrathiaanthracene and Aromatic Dianhydrides. *Macromolecules* **2008**, *41* (17), 6361−6366.

(10) Fukuzaki, N.; Higashihara, T.; Ando, S.; Ueda, M. Synthesis and Characterization of Highly Refractive Polyimides Derived from Thiophene-Containing Aromatic Diamines and Aromatic Dianhydrides. *Macromolecules* **2010**, *43* (4), 1836−1843.

(11) Fu, M.-C.; Murakami, Y.; Ueda, M.; Ando, S.; Higashihara, T. Synthesis and Characterization of Alkaline-Soluble Triazine-Based Poly(Phenylene Sulfide)s with High Refractive Index and Low Birefringence. *J. Polym. Sci. Part A Polym. Chem.* **2018**, *56* (7), 724−731.

(12) Wang, X.; Li, B.; Peng, J.; Wang, B.; Qin, A.; Tang, B. Z. Multicomponent Polymerization of Alkynes, Isocyanides, and Isocyanates toward Heterocyclic Polymers. *Macromolecules* **2021**, *54* (14), 6753−6761.

(13) Fang, L.; Sun, J.; Chen, X.; Tao, Y.; Zhou, J.; Wang, C.; Fang, Q. Phosphorus- and Sulfur-Containing High-Refractive-Index Polymers with High T_g and Transparency Derived from a Bio-Based Aldehyde. *Macromolecules* **2020**, *53* (1), 125−131.

(14) Watanabe, S.; Takayama, T.; Nishio, H.; Matsushima, K.; Tanaka, Y.; Saito, S.; Sun, Y.; Oyaizu, K. Synthesis of Colorless and High-Refractive-Index Sulfoxide-Containing Polymers by the Oxidation of Poly(Phenylene Sulfide) Derivatives. *Polym. Chem.* **2022**, *13* (12), 1705−1711.

(15) Suzuki, Y.; Murakami, K.; Ando, S.; Higashihara, T.; Ueda, M. Synthesis and Characterization of Thianthrene-Based Poly(Phenylene Sulfide)s with High Refractive Index over 1.8. *J. Mater. Chem.* **2011**, *21* (39), 15727.

(16) Kotaki, T.; Nishimura, N.; Ozawa, M.; Fujimori, A.; Muraoka, H.; Ogawa, S.; Korenaga, T.; Suzuki, E.; Oishi, Y.; Shibasaki, Y. Synthesis of Highly Refractive and Highly Fluorescent Rigid Cyanuryl Polyimines with Polycyclic Aromatic Hydrocarbon Pendants. *Polym. Chem.* **2016**, *7* (6), 1297−1308.

(17) Kim, H.; Ku, B.-C.; Goh, M.; Ko, H. C.; Ando, S.; You, N.-H. Synergistic Effect of Sulfur and Chalcogen Atoms on the Enhanced Refractive Indices of Polyimides in the Visible and Near-Infrared Regions. *Macromolecules* **2019**, *52* (3), 827−834.

(18) Gao, Q.; Xiong, L. H.; Han, T.; Qiu, Z.; He, X.; Sung, H. H. Y.; Kwok, R. T. K.; Williams, I. D.; Lam, J. W. Y.; Tang, B. Z. Three-Component Regio- And Stereoselective Polymerizations toward Functional Chalcogen-Rich Polymers with AIE-Activities. *J. Am. Chem. Soc.* **2019**, *141* (37), 14712−14719.

(19) Wu, X.; He, J.; Hu, R.; Tang, B. Z. Room-Temperature Metal-Free Multicomponent Polymerizations of Elemental Selenium toward Stable Alicyclic Poly(Oxaselenolane)s with High Refractive Index. *J. Am. Chem. Soc.* **2021**, *143* (38), 15723−15731.

(20) Griebel, J. J.; Namnabat, S.; Kim, E. T.; Himmelhuber, R.; Moronta, D. H.; Chung, W. J.; Simmonds, A. G.; Kim, K. J.; Van Der Laan, J.; Nguyen, N. A.; Dereniak, E. L.; MacKay, M. E.; Char, K.; Glass, R. S.; Norwood, R. A.; Pyun, J. New Infrared Transmitting Material via Inverse Vulcanization of Elemental Sulfur to Prepare High Refractive Index Polymers. *Adv. Mater.* **2014**, *26* (19), 3014−3018.

(21) Kleine, T. S.; Nguyen, N. A.; Anderson, L. E.; Namnabat, S.; Lavilla, E. A.; Showghi, S. A.; Dirlam, P. T.; Arrington, C. B.; Manchester, M. S.; Schwiegerling, J.; Glass, R. S.; Char, K.; Norwood, R. A.; Mackay, M. E.; Pyun, J. High Refractive Index Copolymers with Improved Thermomechanical Properties via the Inverse Vulcanization of Sulfur and 1,3,5-Triisopropenylbenzene. *ACS Macro Lett.* **2016**, *5* (10), 1152−1156.

(22) Kim, D. H.; Jang, W.; Choi, K.; Choi, J. S.; Pyun, J.; Lim, J.; Char, K.; Im, S. G. One-Step Vapor-Phase Synthesis of Transparent High Refractive Index Sulfur-Containing Polymers. *Sci. Adv.* **2020**, *6* (28), No. eabb5320.

(23) Jang, W.; Choi, K.; Choi, J. S.; Kim, D. H.; Char, K.; Lim, J.; Im, S. G. Transparent, Ultrahigh-Refractive Index Polymer Film ($n \sim 1.97$) with Minimal Birefringence ($\Delta n < 0.0010$). *ACS Appl. Mater. Interfaces* **2021**, *13* (51), 61629−61637.

(24) Watanabe, S.; Oyaizu, K. Designing Ultrahigh-Refractive-Index Amorphous Poly(Phenylene Sulfide)s Based on Dense Intermolecular Hydrogen-Bond Networks. *Macromolecules* **2022**, *55* (6), 2252−2259.
(25) Yamamoto, K.; Tsuchida, E.; Nishide, H.; Jikei, M.; Oyaizu, K. Oxovanadium-Catalyzed Oxidative Polymerization of Diphenyl Disulfides with Oxygen. *Macromolecules* **1993**, *26* (13), 3432−3437.
(26) Yamamoto, K.; Jikei, M.; Katoh, J.; Nishide, H.; Tsuchida, E. Synthesis of Poly(Arylene Sulfide)s by Cationic Oxidative Polymerization of Diaryl Disulfides. *Macromolecules* **1992**, *25* (10), 2698−2704.
(27) Watanabe, S.; Oyaizu, K. Methoxy-Substituted Phenylenesulfide Polymer with Excellent Dispersivity of TiO_2 Nanoparticles for Optical Application. *Bull. Chem. Soc. Jpn.* **2020**, *93* (11), 1287−1292.
(28) Otsuka, H.; Nagano, S.; Kobashi, Y.; Maeda, T.; Takahara, A. A Dynamic Covalent Polymer Driven by Disulfidemetathesis under Photoirradiation. *Chem. Commun.* **2010**, *46* (7), 1150−1152.
(29) Nakai, Y.; Takahashi, A.; Goseki, R.; Otsuka, H. Facile Modification and Fixation of Diaryl Disulphide-Containing Dynamic Covalent Polyesters by Iodine-Catalysed Insertion-like Addition Reactions of Styrene Derivatives to Disulphide Units. *Polym. Chem.* **2016**, *7* (28), 4661−4666.
(30) Watanabe, S.; Oyaizu, K. Catechol End-Capped Poly(Arylene Sulfide) as a High-Refractive-Index "TiO_2/ZrO_2-Nanodispersible" Polymer. *ACS Appl. Polym. Mater.* **2021**, *3* (9), 4495−4503.
(31) Sato, Y.; Sobu, S.; Nakabayashi, K.; Samitsu, S.; Mori, H. Highly Transparent Benzothiazole-Based Block and Random Copolymers with High Refractive Indices by RAFT Polymerization. *ACS Appl. Polym. Mater.* **2020**, *2* (8), 3205−3214.
(32) Nambu, Y.; Yoshitake, Y.; Yanagi, S.; Mineyama, K.; Tsurui, K.; Kuwata, S.; Takata, T.; Nishikubo, T.; Ishikawa, K. Dinaphtho[2,1-*b*:1′,2′-d]Thiophenes as High Refractive Index Materials Exploiting the Potential Characteristics of "Dynamic Thiahelicenes. *J. Mater. Chem. C* **2022**, *10* (2), 726−733.

https://doi.org/10.1021/acspolymersau.2c00030
ACS Polym. Au 2022, 2, 458−466